UNITED NATIONS EDUCATIONAL, SCIENTIFIC AND CULTURAL ORGANIZATION
INTERNATIONAL ATOMIC ENERGY AGENCY
INTERNATIONAL CENTRE FOR THEORETICAL PHYSICS
I.C.T.P., P.O. BOX 586, 34100 TRIESTE, ITALY, CABLE: CENTRATOM TRIESTE

SMR/989 - 16

"Course on Shallow Water and Shelf Sea Dynamics"
7 - 25 April 1997

"Topographic Modes of the Cilician Basin"

E. OZSOY
Middle East Technical University
Institute of Marine Sciences
Icel
Turkey

Please note: These are preliminary notes intended for internal distribution only.

K/ZILKAYA, 1984

TOPOGRAPHIC MODES OF THE CILICIAN BASIN

II. FORMULATION

Integration of the momentum and continuity equations for incompressible fluid motion over the depth results in the governing hydrodynamic equations that we choose to investigate in this study.

2.1 The governing Equations

A uniformly rotating two-layer fluid in a channel of variable depth is assumed on an f-plane in the northern hemisphere. The motion in each layer is assumed to be hydrostatic and independent of the vertical coordinate(Fig. 2.1).

The linear momentum and continuity equations are:

$$\frac{\partial \vec{U}_1}{\partial t} + f\hat{k} \times \vec{U}_1 = -\frac{1}{\rho_1}\nabla p_1 \qquad (2.1.1)$$

$$\frac{\partial \vec{U}_2}{\partial t} + f\hat{k} \times \vec{U}_2 = -\frac{1}{\rho_2}\nabla p_2 \qquad (2.1.2)$$

$$\frac{\partial (\eta_1-\eta_2)}{\partial t} + \nabla . H_1 \vec{U}_1 = 0 \qquad (2.1.3)$$

$$\frac{\partial \eta_2}{\partial t} + \nabla . H_2 \vec{U}_2 = 0 \qquad (2.1.4)$$

where the subscripts 1 and 2 denote the upper and lower layer, respectively.

The hydrostatic pressure in each layer is given by

$$p_1 = \rho_1 g(\eta_1 - z) \qquad (2.1.5)$$

$$p_2 = \rho_1 g(\eta_1 - \eta_2 + H_1) + \rho_2 g(\eta_2 - H_1 - z) \qquad (2.1.6)$$

Equations (2.1.1-2.1.4) are non-dimensionalized by introducing the following scaling relations:

$$\begin{aligned} &u_j \sim U_o, \quad j=1,2 \\ &H_j \sim H_o, \quad j=1,2 \\ &\eta_1 \sim \frac{fU_oW}{g} \\ &\eta_2 \sim \frac{fU_oW}{g\Delta\rho/\rho_2} \\ &(x,y) \sim W \end{aligned} \qquad (2.1.7)$$

where W, H_o are the characteristic length and depth scales, respectively. U_o is the characteristic velocity scale, and $\Delta\rho = \rho_2 - \rho_1$ is the density difference between layers. For the Cilician Basin located at 36° latitute, the Coriolis parameter is given as $f = 8.55 \times 10^{-5}$ radian.sec^{-1}.

Introducting (2.1.5), (2.1.6) and (2.1.7) into (2.1.1-2.1.4) the non-dimensional form of the momentum and continuity equations are

$$\frac{\partial \vec{U}_1}{\partial t} + \hat{k} \times \vec{U}_1 = -\nabla \eta_1 \qquad (2.1.8)$$

$$\frac{\partial \vec{U}_2}{\partial t} + \hat{k} \times \vec{U}_2 = -\nabla \eta_2 - \nabla(\eta_2 - \frac{\Delta\rho}{\rho_2}\eta_1) \qquad (2.1.9)$$

$$\delta_E \frac{\partial \eta_1}{\partial t} - \delta_I \frac{\partial \eta}{\partial t} + \nabla . H_1 \vec{U}_1 = 0 \qquad (2.1.10)$$

$$\delta_I \frac{\partial \eta_2}{\partial t} + \nabla . H_2 \vec{U}_2 = 0 \qquad (2.1.11)$$

where $\delta_E = \frac{f^2 W^2}{g H_o}$ and $\delta_I = \frac{f^2 W^2}{g H_o (\Delta\rho/\rho_2)}$

η_1 and η_2 are disturbances of free surface and interface. H_1 and H_2 the mean layer thickness respectively, and $\vec{U}_j$, $j = 1,2$ the average velocity in each layer.

We now introduce new variables in the following form:

$$\begin{aligned} \vec{U} &= \vec{U}_2 - \vec{U}_1 \\ \vec{m} &= H_1 \vec{U}_1 + H_2 \vec{U}_2 \\ \eta &= \eta_2 - \frac{\Delta\rho}{\rho_2}\eta_1 \\ \lambda &= \eta_1 \\ H &= H_1 + H_2 \end{aligned} \qquad (2.1.12)$$

and reduce equations (2.1.8)-(2.1.9) using (2.1.10) in the following steps:

Combining (2.1.8) and (2.1.9) after multiplying each by the layer thicknesses H_1 and H_2 yields

$$\frac{\partial \vec{m}}{\partial t} + \hat{k} \times \vec{m} = -H\nabla\lambda - H_2\nabla\eta \qquad (2.1.13)$$

Taking the divergence of (2.1.13) and utilizing (2.1.10), (2.1.11) and (2.1.12) we have

$$-\delta_E \frac{\partial^2 \lambda}{\partial t^2} - \hat{k}.(\nabla \times \vec{m}) = -\nabla.(H\nabla\lambda + H_2\nabla\eta) \qquad (2.1.14)$$

Differentiating (2.1.14) yields

$$-\frac{\partial}{\partial t}\nabla.(H\nabla\lambda + H_2\nabla\eta) - \delta_E \frac{\partial^3 \lambda}{\partial t^3} = \hat{k}.\frac{\partial}{\partial t}\nabla \times \vec{m} \qquad (2.1.15)$$

Whereas the curl of (2.1.13) gives

$$\hat{k}.\frac{\partial}{\partial t}\nabla \times \vec{m} - \delta_E \frac{\partial \lambda}{\partial t} = \nabla H.(\hat{k} \times \nabla\lambda) + \nabla H_2.(\hat{k} \times \nabla\eta) \qquad (2.1.16)$$

Eliminating $\vec{m}$ between (2.1.15) and (2.1.16), we obtain the following equation for variables λ and η:

$$\frac{\partial}{\partial t}\left[\nabla.(H\nabla\lambda + H_2\nabla\eta) - \delta_E \mathcal{L}(\lambda)\right] - \nabla H.(\hat{k} \times \nabla\lambda) - \nabla H_2.(\hat{k} \times \nabla\eta) = 0 \qquad (2.1.17)$$

where $\mathcal{L}(.) = \frac{\partial^2(.)}{t^2} + 1(.)$.

After multiplying equation (2.1.10) by $-\frac{1}{H_1}$ and equation (2.1.11) by $\frac{1}{H_2}$ and adding these, we obtain

$$\nabla.\vec{U} = \frac{1}{H}\vec{U}.\nabla H_1 - \frac{1}{H_2}\vec{U}_2 .\nabla H_2 - \delta_E \frac{H}{H_1 H_2}\frac{\partial \eta}{\partial t} - \delta_E \frac{1}{H_2}\frac{\partial \lambda}{\partial t} \qquad (2.1.18)$$

Now, let $\mathcal{L}(.)$ operate on equation (2.1.18) :

$$\mathcal{L}(\nabla.\vec{U}) = -\frac{\partial}{\partial t}\left[\delta_1 \frac{H}{H_1 H_2}\mathcal{L}(\eta) + \delta_E \frac{1}{H_2}\mathcal{L}(\lambda)\right] + \frac{\nabla H_1}{H_1}\mathcal{L}(\vec{U}_1) - \frac{\nabla H_2}{H_2}\mathcal{L}(\vec{U}_2) \qquad (2.1.19)$$

It is straightforward to show that some manipulation of (2.1.8) leads to

$$\mathcal{L}(\vec{U}_1) = -\frac{\partial}{\partial t}\nabla\lambda + \hat{k} \times \nabla\lambda \qquad (2.1.20)$$

and of (2.1.19) leads to

$$\mathcal{L}(\vec{U}_2) = -\frac{\partial}{\partial t}\nabla\lambda + \hat{k} \times \nabla\lambda - \frac{\partial}{\partial t}\nabla\eta + \hat{k} \times \nabla\eta \qquad (2.1.21)$$

It can also be shown that the sub‸traction of (2.1.8) from (2.1.9) yields

$$\frac{\partial \vec{U}}{\partial t} + \hat{k} \times \vec{U} = -\nabla\eta \qquad (2.1.22)$$

First by taking the curl of (2.1.22) and then the derivative of the divergence of the same equation one can also obtain

$$\mathcal{L}(\nabla.\vec{U}) = -\frac{\partial}{\partial t}\nabla^2\eta \qquad (2.1.23)$$

Now, making use of (2.1.20), (2.1.21) and (2.1.23) in (2.1.19) results in the following equation.

$$\frac{\partial}{\partial t}\left[\nabla^2\eta - \delta_1 \frac{H}{H_1 H_2}\mathcal{L}(\eta) - \delta_E \frac{1}{H_2}\mathcal{L}(\lambda) - \frac{H}{H_1 H_2}\nabla H_1 .\nabla\lambda + \frac{1}{H_2}\nabla H.\nabla\lambda + \frac{\nabla H_2}{H_2}.\nabla\eta\right] + \frac{H}{H_1 H_2}\nabla H_1 .\ \hat{k} \times \nabla\lambda - \frac{\nabla H}{H_2}\hat{k} \times \nabla\lambda - \frac{\nabla H_2}{H_2}\hat{k} \times \nabla\lambda - \frac{\nabla H_2}{H_2}\hat{k} \times \nabla\eta = 0 \qquad (2.1.24)$$

Multiplying (2.1.24) by H_2 and substracting from (2.1.17) yields

$$\frac{\partial}{\partial t}\left[\nabla.(H_1\nabla\lambda) + \delta_1\mathcal{L}(\eta)\right] - \nabla H_1 .\hat{k} \times \nabla\lambda = 0 \qquad (2.1.25)$$

Equations (2.1.17) and (2.1.25) constitute, two coupled differential equations for solving λ and η. The coupled equations (2.1.17) and (2.1.25) will be used to model the free motions in a uniform channel geometry. The depth variations are assumed to be present in only the cross-channel direction (x), while the depth variations

in the along channel direction are neglected.
The Cilician Basin can quite closely be modelled by such a geometry since the channel is almost straight with the more significant depth variations taking place across the basin. The length of the channel L is typically three times larger than its width W to allow sufficient distance for uniform propagation along the basin.

For propagating wave solutions in the along channel direction (Y), we assume solutions of the form

$$\lambda = L(x)e^{i(ky-wt)} \qquad (2.1.26)$$

$$\eta = N(x)e^{i(ky-wt)} \qquad (2.1.27)$$

$$\vec{U}_j = \vec{U}_j(x)e^{i(ky-wt)} \quad , \quad j = 1,2 \qquad (2.1.28)$$

where w is the wave frequency, k the long channel wave number and $L(x)$, $N(x)$ and $\vec{U}_j(x)$ are amplitude functions. The vector velocity amplitude has components $U_j = (u_j, v_j)$ in each layer, j=1,2 .

The dimensional frequency w' and wavenumber k' are respectively related to the dimensionless frequency and wavenumber by

$$w' = fw$$
$$k' = k/W \qquad (2.1.29)$$

The horizontal length scale W is taken to be the distance between south coast of Turkey and north coast of Cyprus. In Figure (2.1) the channel width has a typical value of W = 100 km. Substituting (2.1.26) and (2.1.27) into equations (2.1.17) and (2.1.25) yields the following equations:

$$\frac{d^2 L}{dx} - k^2 L + \frac{\delta_1(1-w^2)}{H_1} N = 0 \qquad (2.1.30)$$

$$\frac{d}{dx}\left(H\frac{dL}{dx}\right) - \left[k^2 H + \frac{k}{w}\frac{dH}{dx} + \delta_\varepsilon(1-w^2)\right] + \frac{d}{dx}\left(H_2\frac{dN}{dx}\right)$$
$$- \left(k^2 H_2 + \frac{k}{w}\frac{dH_2}{dx}\right) N = 0 \qquad (2.1.31)$$

in which the upper layer is assumed to be of constant thickness (H_1 = constant).

The normal velocity components U_1 and U_2 at the boundaries x = 0,1 must satisfy the boundary conditions

$$U_1 = \hat{1}\cdot\vec{U}_1 = 0 \qquad \text{on } x = 0,1 \qquad (2.1.32)$$

$$U_2 = \hat{1}\cdot\vec{U}_2 = 0 \qquad \text{on } x = 0,1 \qquad (2.1.33)$$

The velocity in each layer is given by (2.1.20) and (2.1.21). The velocity amplitudes are likewise obtained by substitution from (2.1.26)-(2.1.28). The boundary conditions (2.1.31) and (2.1.32) are equivalent to require the x-component velocity

$U_j = 0,\ j = 1,2$ in the relations (cf. 2.1.20 and 2.1.21) which yield

$$\frac{dL}{dx} - \frac{k}{w}L = 0 \quad \text{on} \quad x = 0,1 \qquad (2.1.34)$$

$$\frac{dN}{dx} - \frac{k}{w}N = 0 \quad \text{on} \quad x = 0,1 \qquad (2.1.35)$$

as boundary conditions for (2.1.30) and (2.1.31).

The above equations are simplified considerably if we make the change of the variables

$$M = L + N \qquad (2.1.36)$$

which by virtue of (2.1.26), (2.1.27) and (2.1.12) is equivalent to

$$\eta_2 + \left(1 - \frac{\Delta\rho}{\rho_2}\right)\eta_1 = \eta + \lambda = M(x)e^{i(ky-wt)} \equiv \mu \qquad (2.1.37)$$

With (2.1.36) and $H = H_1 + H_2$ equations (2.1.30), (2.1.31), (2.1.34) and (2.1.35) take the following form

$$M_{xx} + \frac{H_{2x}}{H_2} M_x - \left[k^2 + \frac{k}{w}\frac{H_{2x}}{H_2} + \frac{\delta_1(1-w^2)}{H_2}\right] M + \left[\frac{(\delta_1 - \delta_E)(1-w^2)}{H_2}\right] L = 0 \qquad (2.1.38)$$

$$L_{xx} - k^2 L + \frac{\delta_1(1-w^2)}{H}(M-L) = 0 \qquad (2.1.39)$$

$$M_x - \frac{k}{w}M = 0 \qquad \text{on } x = 0,1 \qquad (2.1.40)$$

$$L_x - \frac{k}{w}L = 0 \qquad \text{on } x = 0,1 \qquad (2.1.41)$$

where the subscript x denotes differentiation.

The velocity amplitude components can be obtained by substitution of (2.1.26-2.1.28) into (2.1.20) and (2.1.21). Making use of (2.1.36) the components in each layer are calculated from:

$$U_1 = \frac{1}{1-w^2}(iwL_x - ikL) \qquad (2.1.42)$$

$$V_1 = \frac{1}{1-w^2}(L_x - wkL) \qquad (2.1.43)$$

$$U_2 = \frac{1}{1-w^2}(iwM_x - ikM) \qquad (2.1.44)$$

$$V_2 = \frac{1}{1-w^2}(M_x - wkM) \qquad (2.1.45)$$

2.2 Approximate Solution for Free Modes in a Channel with Exponential Depth Profile

The system (2.1.38-2.1.41) for an exponential bottom with a vertical wall at x=0 has been discussed by several in the context of shelf waves. Considering a channel with an exponential bottom profile, approximate solutions with $H_1 \ll H_2$ will be used here to demostrate certain characteristics of free motions. The solutions were further used for checking the consistency of numerical solutions.

We consider the free oscillations in a channel of width 1, where the lower layer depth is specified as

$$H_2(x) = e^{2b(x-1)} \qquad (2.2.1)$$

such that $H_2(0) = e^{-2b}$ and $H_2(1) = 1$. With substitutions

$$r(x) = \frac{H_{2x}}{H_2}$$

$$\ell(x) = \frac{H_1}{H_2}$$

$$\mu_I = \frac{\delta_I(1-w^2)}{H_1} \qquad (2.2.2)$$

$$\mu_E = \frac{\delta_E(1-w^2)}{H_1}$$

$$\lambda = \frac{k}{w}$$

equations (2.1.38 - 2.1.41) can be written as

$$L_{xx} - k^2 L + \mu_I(M-L) = 0 \qquad (2.2.3)$$

$$M_{xx} + rM_x - (k^2 + \lambda r + \ell \mu_I)M + (\mu_I - \mu_E) L = 0 \qquad (2.2.4)$$

$$L_x - \lambda L = 0 \qquad (2.2.5)$$

$$M_x - \lambda M = 0 \qquad (2.2.6)$$

In seeking an approximate solution to (2.2.3 - 2.3.6) we make the assumptions

$\ell \ll 1$, since $H_1 \ll H_2$ $\qquad \mu_E \ll \mu_I$ since $\delta_E \ll \delta_I$

With these approximations, the eigenvalue problem is simplified to

$$L_{xx} - k^2 L + \mu_I(M-L) = 0 \qquad (2.2.7)$$

$$M_{xx} + 2bM_x - (k + 2b\lambda) M = 0 \qquad (2.2.8)$$

$$M_x - \lambda M = 0 \quad \text{on } x = 0,1 \qquad (2.2.9)$$

$$L_x - \lambda L = 0 \quad \text{on } x = 0,1 \qquad (2.2.10)$$

where $r = 2b$ has been substituted by virtue of (2.2.1) and (2.2.2). Note that (2.2.8) is now uncoupled from (2.2.7).

The general solution of equations (2.2.7 - 2.2.10) are obtained as

$$L(x) = A_1 e^{l_1 x} + A_2 e^{l_2 x} + B_1 e^{m_1 x} + B_2 e^{m_2 x} \qquad (2.2.11)$$

$$M(x) = C_1 e^{m_1 x} + C_2 e^{m_2 x} \qquad (2.2.12)$$

for which the characteristic equations are

$$l^2 - k^2 - \mu_1 = 0 \tag{2.2.13}$$

$$m^2 + 2bm - (k^2+2b\lambda) = 0 \tag{2.2.14}$$

and the roots are

$$l_{1,2} = \mp\sqrt{k^2+\mu_1} \equiv \mp q \tag{2.2.15}$$

$$m_{1,2} = -b \mp\sqrt{b^2+k^2+2b\lambda} \equiv -b \mp p \tag{2.2.16}$$

The boundary conditions (2.2.9) yield two linear homogenous equations for C_1 and C_2, i.e.

$$(m_1-\lambda)\ C_1 + (m_2-\lambda)\ C_2 = 0 \tag{2.2.17}$$

$$e^{m_1}(m_1-\lambda)\ C_1 + e^{m_2}(m_2-\lambda)\ C_2 = 0 \tag{2.2.18}$$

A nontrivial solution of (2.2.17) and (2.2.18) requires by making use of (2.2.16) that

$$(m_1-\lambda)\ (m_2-\lambda)\ e^{-b}\ 2\sinh p = 0 \tag{2.2.19}$$

The only nontrival case satisfying (2.2.19) occurs when p has an imaginary value, i.e., $p=ip'$ (p' is real), satisfying

$$\sinh p = i\sin p' = 0$$

or

$$p' = n\Pi \tag{2.2.20}$$

where n is an integer. Since in (2.2.16)

$$p = \sqrt{b^2+k^2+2b\lambda} = ip' \tag{2.2.21}$$

and

$$(p')^2 = -(b^2+k^2+2b\lambda) = (n\Pi)^2 \tag{2.2.22}$$

by virtue of (2.2.20), the dispersion relation is obtained as

$$w = -\frac{2bk}{b^2+k^2+(n\Pi)^2} \qquad n=1,2,3,\ldots \tag{2.2.23}$$

It can be verified that the integer value n=0 should not be included in the modes, since this results in $p'=0$ or $m=-b$ as a single root, for which the solution would not satisfy the boundary conditions.

To obtain the eigenfunction M(x), the equations (2.2.21) and (2.2.16) are substituted in (2.2.12) to give

$$M(x) = e^{-bx}\ (C_1 e^{in\Pi x} + C_2 e^{-in\Pi x}) \tag{2.2.24}$$

The relation between C_1 and C_2 are given by (2.2.17) as

$$C_2 = -C_1 \frac{(-b+in\Pi-\lambda)}{(-b-in\Pi-\lambda)} \tag{2.2.25}$$

Now introducing

$$p = b^2 - k^2 - (n\pi)^2 \qquad q = 2bn\pi \tag{2.2.26}$$

and utilizing (2.2.22), we obtain

$$M(x) = Ce^{-bx}\,(p\sin n\pi x + q\cos n\pi x) \tag{2.2.27}$$

where C is an arbitrary constant such that

$$C = \frac{2C_1}{q-ip} = \frac{2C_2}{q+ip} \tag{2.2.28}$$

To obtain the eigenfunction L(x), we first write (2.2.11) as

$$L(x) = A_1 e^{qx} + A_2 e^{-qx} + B_1' e^{-bx}\sin n\pi x + B_2' e^{-bx}\cos n\pi x \tag{2.2.29}$$

by making use of (2.2.15), (2.2.16) and (2.2.21). The inhomogenous part of L, i.e.,

$$\hat{L}(x) = B_1' e^{-bx}\sin n\pi x + B_2' e^{-bx}\cos n\pi x \tag{2.2.30}$$

should satisfy equation (2.2.7). Substituting (2.2.30) and (2.2.27) into equation(2.2.7), we obtain

$$B_1'\left[b^2 - (n\pi)^2 + 2bn\pi - (k^2+\mu_1)\right] + \mu_1 C_1 = 0 \tag{2.2.31}$$

$$B_2'\left[b^2 - (n\pi)^2 - 2bn\pi - (k^2+\mu_1)\right] + \mu_1 C_2 = 0 \tag{2.2.32}$$

On the other hand, the boundary conditions (2.2.5) applied for (2.2.29) yield,

$$A_1(q-\lambda) + A_2(q-\lambda) + B_1'(-b+n\pi) = 0 \tag{2.2.33}$$

$$A_1(q-\lambda) + A_2(q-\lambda) + B_2'(-b+n\pi) = 0 \tag{2.2.34}$$

Solving (2.2.31 - 2.2.34) for the unknown coefficients, utilizing (2.2.28) yields:

$$\begin{aligned} B_1 &= -\frac{\mu_1 p}{r+q}\,C \\ B_2 &= -\frac{\mu_1 p}{r-q}\,C \\ A_1 &= \frac{((-1)^n e^{-b} - e^{-q})K}{q-\lambda}\,C \\ A_2 &= \frac{((-1)^n e^{-b} - e^{q})K}{q+\lambda}\,C \end{aligned} \tag{2.2.35}$$

where

$$r = p - \mu_1 \tag{2.2.36}$$

and

$$K = \frac{(n\pi-\lambda)q\mu_1}{2\,\mathrm{sh}\,q\,(r-q)} \tag{2.2.37}$$

Therefore the eigenfunction L(x) can be calculated from (2.2.29) as

$$L(x) = C\left[\frac{((-1)^n e^{-b} - e^{-q})}{(q-\lambda)} K e^{qx} + \frac{((-1)^n e^{-b} - e^{+q})}{(q+\lambda)} K e^{-qx} - \frac{\mu_1 p}{r+q} e^{-bx} \sin n\pi x - \frac{\mu_1 q}{r-q} e^{-bx} \cos n\pi x\right] \quad (2.2.38)$$

The velocity amplitude components can be obtained by substitution of (2.2.27) and (2.2.38) into (2.1.42-2.1.45) . The components in each layer are calculated from:

$$U_1 = \frac{i}{1-w^2} C\left[(wq-k)Ae^{qx} - (wq+k)Be^{-qx} + e^{-bx}\Big((w(Eb+Fn\pi)+Ek)\sin n\pi x + (w(-En\pi+Fb)+Fk)\cos n\pi x\Big)\right] \quad (2.2.39)$$

$$V_1 = \frac{1}{1-w^2} C\left[(q-kw)Ae^{qx} - (q+kw)Be^{-qx} + e^{-bx}\Big((Eb+Fn\pi+Ekw)\sin n\pi x + (-En\pi+Fb+Fkw)\cos n\pi x\Big)\right] \quad (2.2.40)$$

$$U_2 = \frac{i}{1-w^2} \cdot C \cdot e^{-bx}\Big\{(w(-bp-qn\pi)-kp)\sin n\pi x + (w(-bq+pn\pi)-kq)\cos n\pi x\Big\} \quad (2.2.41)$$

$$V_2 = \frac{1}{1-w^2} \cdot C \cdot e^{-bx}\Big\{((-bp-qn\pi)-kwp)\sin n\pi x + ((-bq+pn\pi)-kwq)\cos n\pi x\Big\} \quad (2.2.42)$$

where

$$A = \frac{((-1)^n e^{-b} - e^{-q})K}{(q-\lambda)}$$

$$B = \frac{((-1)^n e^{-b} - e^{q})K}{(q+\lambda)}$$

$$E = \frac{\mu_1 p}{r+q}$$

$$F = \frac{\mu_1 q}{r-q}$$

2.3 Surface and Internal Kelvin Wave Modes in a Channel with Constant Depth

Surface and internal Kelvin wave modes for a constant depth channel were used to obtain first approximations to the respective dispersion curves in the numerical calculations for the variable depth channel, since only small modifications in the dispersion curves of these modes.

Solutions for surface and internal Kelvin waves are therefore briefly reviewed in this section.

2.3.1 Surface Kelvin Wave Modes

The non-dimensional form of the momentum and continuity equations for a single layer (homogenous) fluid with a constant depth (H=1) are

$$\frac{\partial \vec{U}}{\partial t} + \hat{k} \times \vec{U} = -\nabla \eta \qquad (2.3.1)$$

$$\delta_\epsilon \frac{\partial \eta}{\partial t} + \nabla . \vec{U} = 0 \qquad (2.3.2)$$

where $\delta_\epsilon = \frac{f^2 W^2}{gH}$

Taking the divergence and curl of (2.3.1) respectively, we obtain

$$\frac{\partial}{\partial t} \nabla . \vec{U} - \hat{k} . \nabla \times \vec{U} = -\nabla^2 \eta \qquad (2.3.3)$$

$$\frac{\partial}{\partial t} \nabla \times \vec{U} + \hat{k} \nabla . \vec{U} = 0 \qquad (2.3.4)$$

combining (2.3.3) and (2.3.4) and utilizing (2.3.2) yields

$$\left(\frac{\partial^2}{\partial t^2} + 1\right) \left(-\delta_\epsilon \frac{\partial \eta}{\partial t}\right) = - \frac{\partial}{\partial t} \nabla^2 \eta \qquad (2.3.5)$$

Substituting $\eta = N(x)e^{i(ky-wt)}$ into (2.3.5), the above equation can be written as

$$N_{xx} - [k^2 + \delta_\epsilon (1-w^2)] N = 0 \qquad (2.3.6)$$

The normal velocity component U at the boundary x=0,1 must satisfy the boundary condition

$$U = \hat{i}\vec{U} = 0 \qquad \text{on } x=0,1 \qquad (2.3.7)$$

Operating on (2.3.1), one can derive

$$\left(\frac{\partial}{\partial t^2} + 1\right)\vec{U} = -\nabla \eta + \hat{k} \times \nabla \eta \qquad (2.3.8)$$

Making use of (2.3.8) in satisfying (2.3.7) yields

$$\frac{\partial N}{\partial x} - \frac{k}{w} N = 0 \qquad \text{on } x=0,1 \qquad (2.3.9)$$

as boundary condition for (2.3.6). The general solution of (2.3.6) is

$$N = Ae^{\alpha_\epsilon x} - Be^{-\alpha_\epsilon x} \qquad (2.3.10)$$

where

$$d_E^2 = k^2 + (1-w^2)\,\delta_E \qquad (2.3.11)$$

and application of the boundary condition (2.3.10) at x=0,1 yields two linear homogenous equations for A and B. i.e.,

$$A(d_E - \frac{k}{w}) + B(-d_E - \frac{k}{w}) = 0 \qquad (2.3.12)$$

$$A(d_E - \frac{k}{w})e^{d_E} + B(-d_E - \frac{k}{w})e^{-d_E} = 0$$

Nontrivial solutions for A and B can be found only if

$$(d_E - \frac{k}{w})\cdot(-d_E - \frac{k}{w})\cdot(e^{-d_E} - e^{d_E}) = 0 \qquad (2.3.13)$$

The only nontrivial solution satisfying (2.3.13) occurs, for

$$d_E = \mp \frac{k}{w} \qquad (2.3.14)$$

so that (2.3.11) yields the dispersion relation

$$w = \mp \delta_E^{-1/2}\cdot k \qquad (2.3.15)$$

In terms of the dimensional frequency w' and the dimensional wavenumber k' (2.3.15) is equivalent to

$$w' = \mp (gH)^{1/2}\cdot k' \qquad (2.3.16)$$

2.3.2 Internal Kelvin Wave Modes

Assuming constant depths in equations (2.1.38) and (2.1.39) and neglecting δ_E, we obtain the following equations

$$M_{xx} - k\,M - \frac{\delta_I(1-w^2)}{H}(M-L) = 0 \qquad (2.3.17)$$

$$L_{xx} - k\,L - \frac{\delta_I(1-w^2)}{H}(L-M) = 0 \qquad (2.3.18)$$

substracting (2.3.17) from (2.3.18) with the change of variables

$$N = M-L \qquad (2.3.19)$$

and introducing

$$b_I^2 = k^2 + \frac{H}{H_1 H_2}(1-w^2)\,\delta_I \qquad (2.3.20)$$

and

$$H = H_1 + H_2 = 1 \qquad (2.3.21)$$

We obtain

$$N_{xx} - b_I^2 N = 0 \qquad (2.3.22)$$

The boundary conditions to be employed (cf. 2.1.40 and 2.1.41) are

$$\frac{\partial N}{\partial x} - \frac{k}{w} N = 0 \quad \text{on } x = 0,1 \qquad (2.3.23)$$

The general solution of equation (2.3.22) is

$$N = Ae^{b_1 x} - Be^{-b_1 x} \qquad (2.3.24)$$

and application of the boundary conditions at x=0,1 yields two linear homogenous equations, for which nontrivial solutions can be found only if

$$(b_1 - \frac{k}{w}).(-b_1 - \frac{k}{w}).(e^{-b_1} - e^{b_1}) = 0 \qquad (2.3.25)$$

The only nontrivial case satisfying (2.3.24) occurs when

$$b_1 = \mp \frac{k}{w} \qquad (2.3.26)$$

and (2.3.26) yields the dispersion relation

$$w = \mp(H_1 H_2/\delta_1)^{1/2} k \qquad (2.3.27)$$

In dimensional terms (primed variables) this is equivalent to

$$w' = \mp(\frac{\Delta\rho}{\rho} g \frac{H_1 H_2}{H})^{1/2} k' \qquad (2.3.28)$$

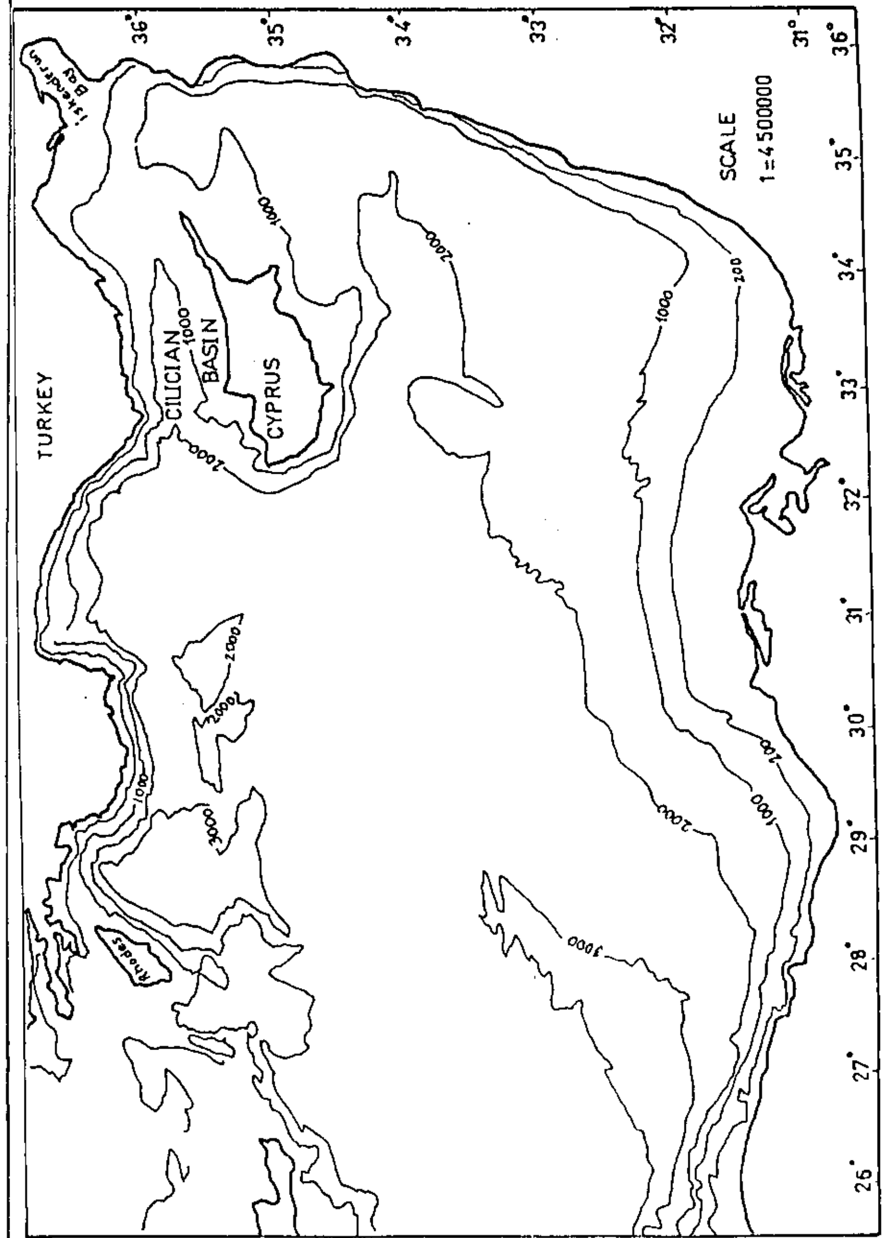

Figure 1.1 Regional Map

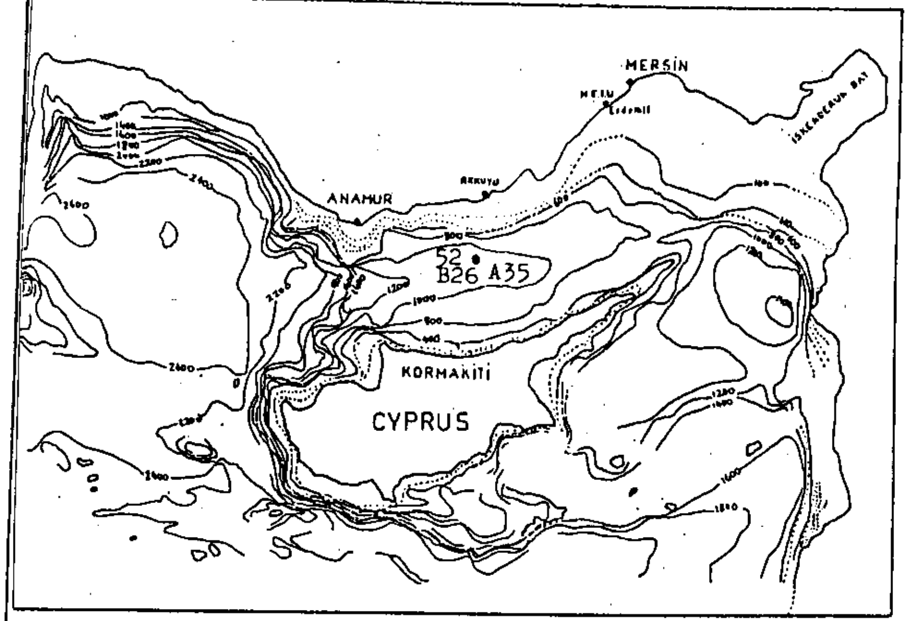

Figure 1.2 The bathymetry of the Cilician basin between the northern coast of Cyprus and southern coast of Turkey.

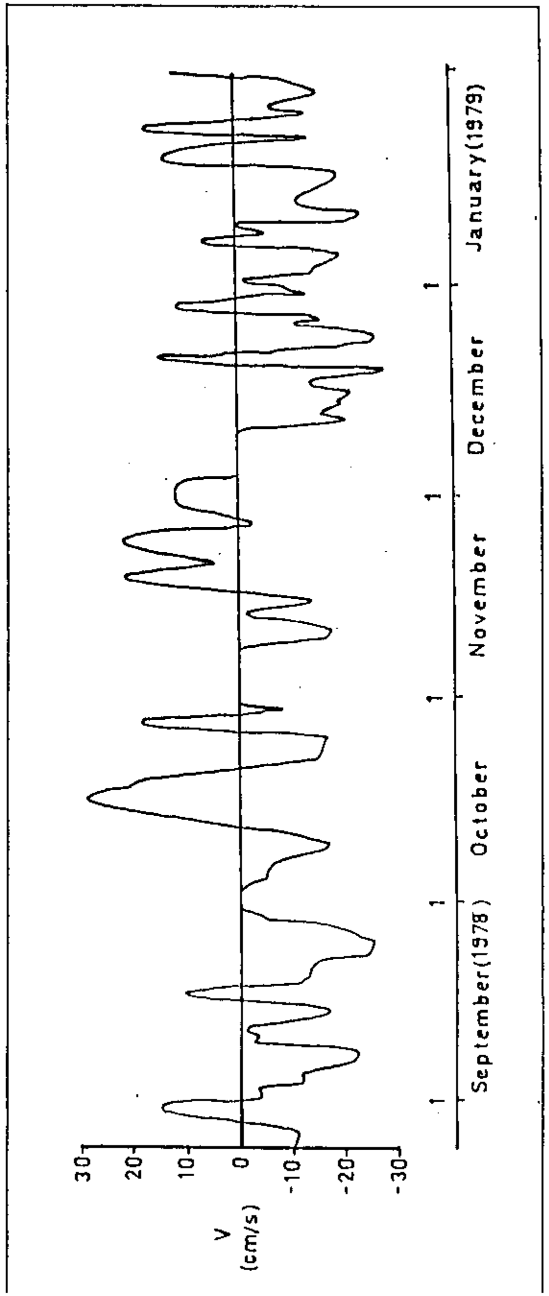

Figure 1.3 Alongshore components of low passed filtered currents during September 1978 - January 1979

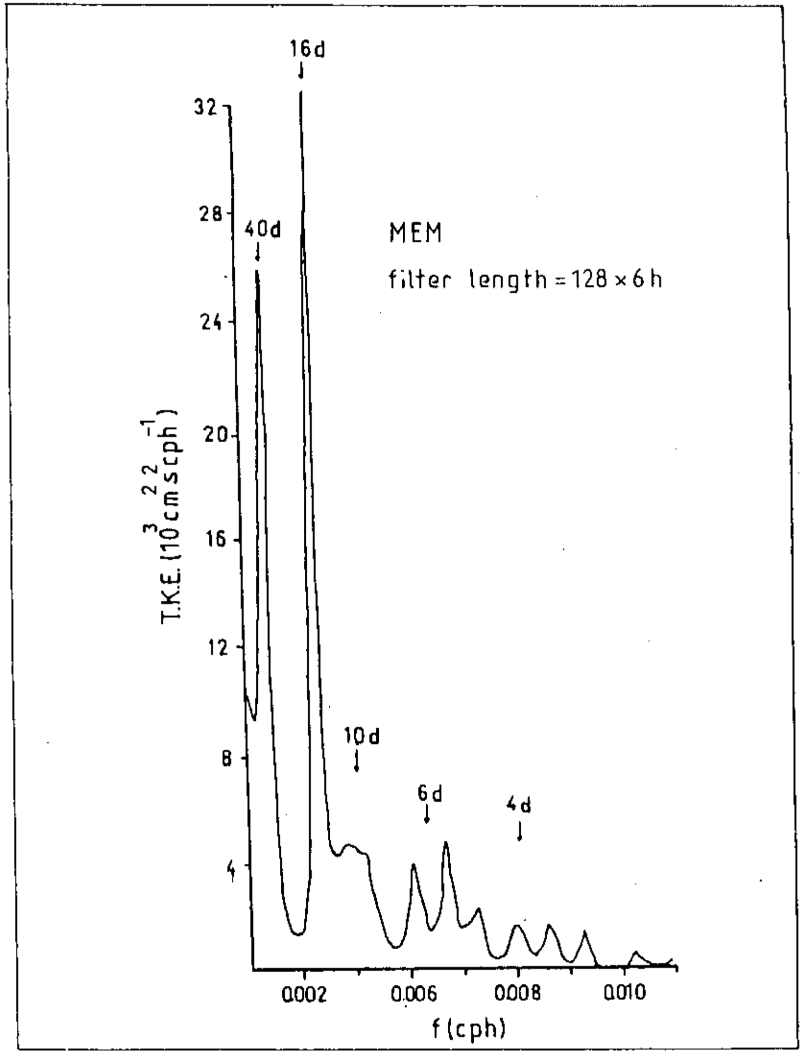

Figure 1.4 MEM and Raw spectra of currents during September 1978 - January 1979

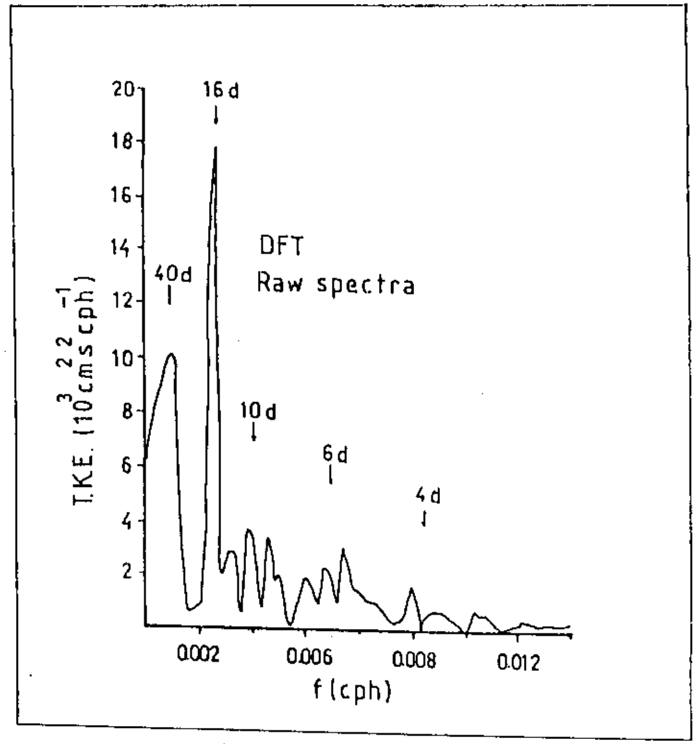

Figure 1.4 Continued

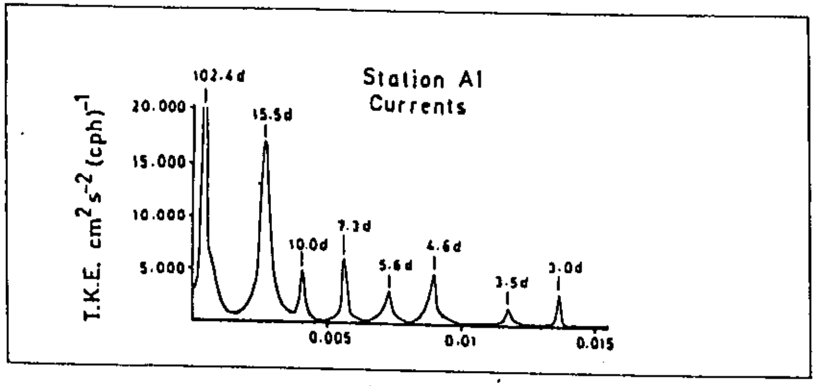

(a)

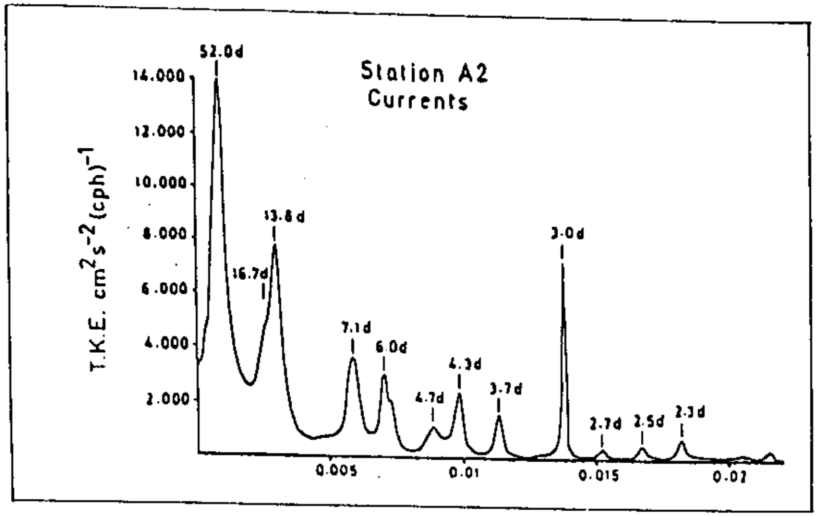

(b)

Figure 1.5 Maximum entropy (MEM) spectra of low passed currents at sites A1 (a), A2 (b), E1 (c), 1980

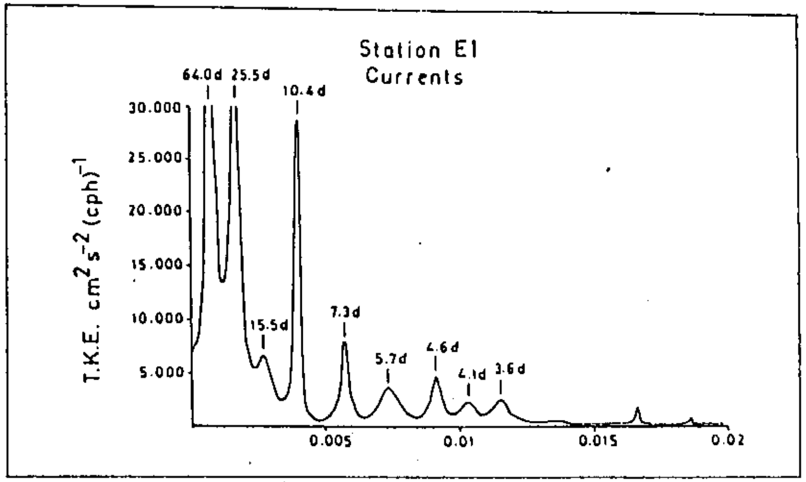

(c)

Figure 1.5 Continued

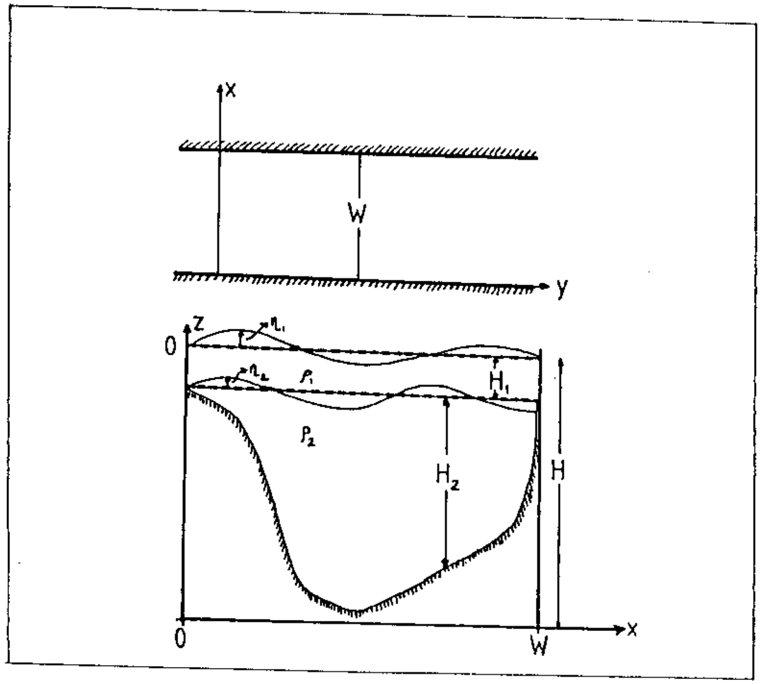

Figure 2.1 Coordinate system chosen. W is the channel width and H is the maximum water depth

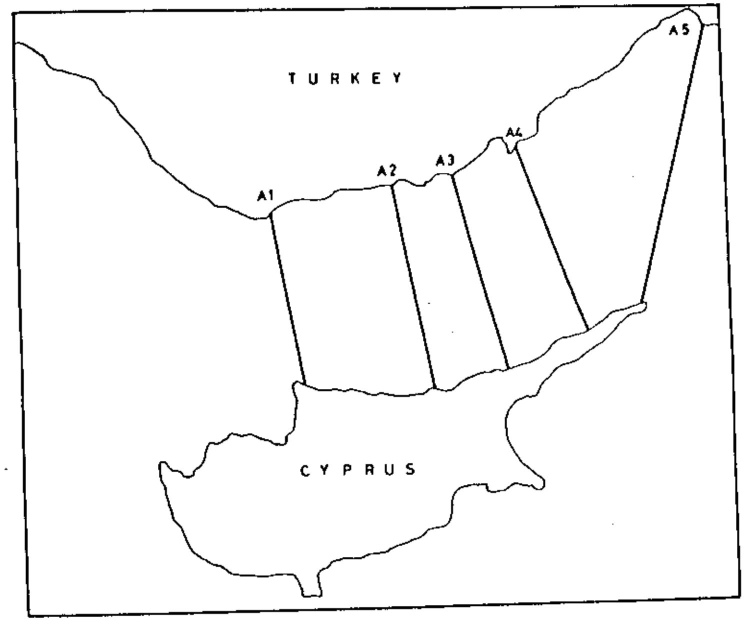

Figure 4.1 Locations of the cross-sections in Cilician basin

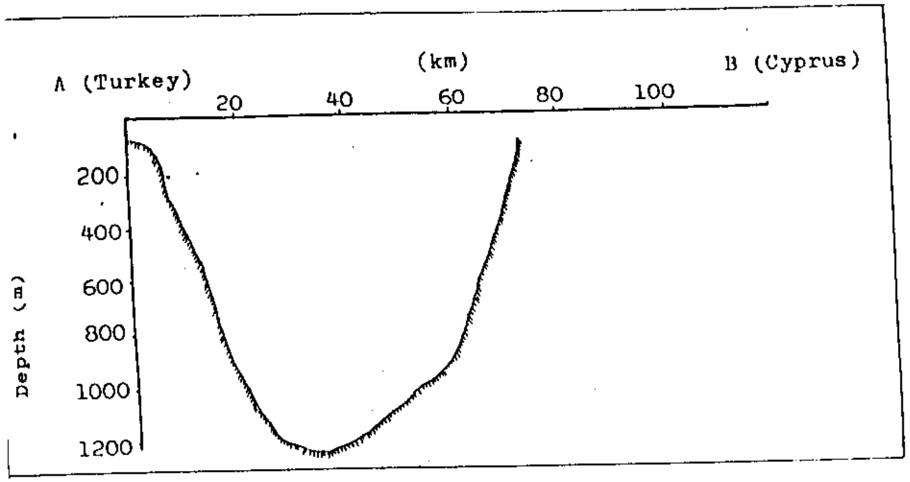

(a)

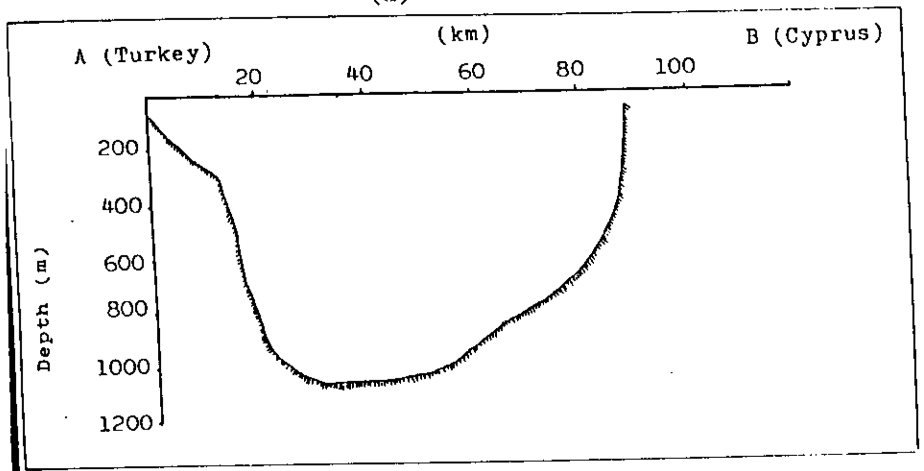

(b)

Figure 4.2 Bottom topography across A1 cross-section (a), A2 cross-section (b), A3 cross-section (c), A4 cross-section (d), A5 cross-section (e)

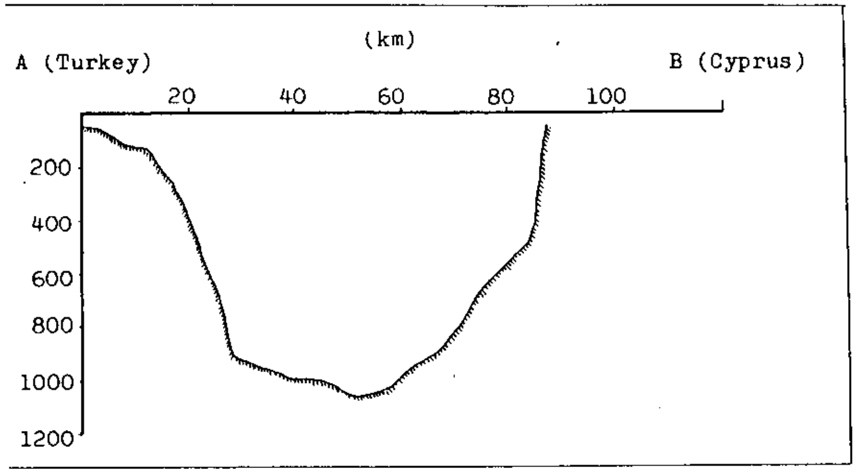

(c)

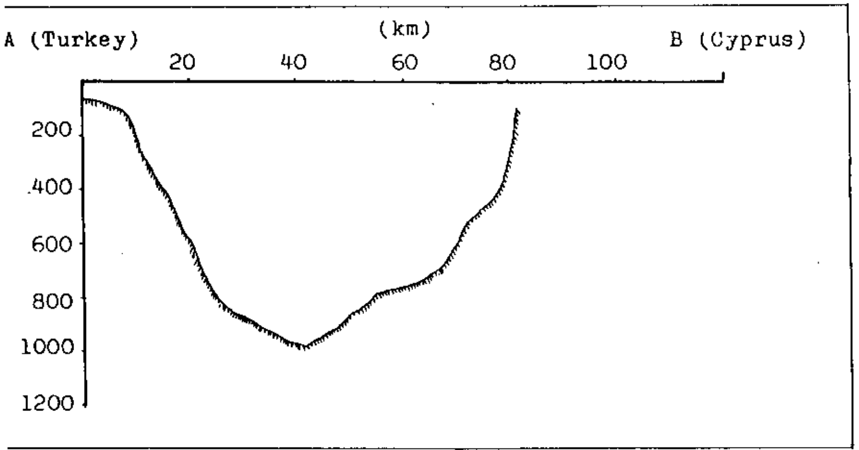

(d)

Figure 4.2 Continued

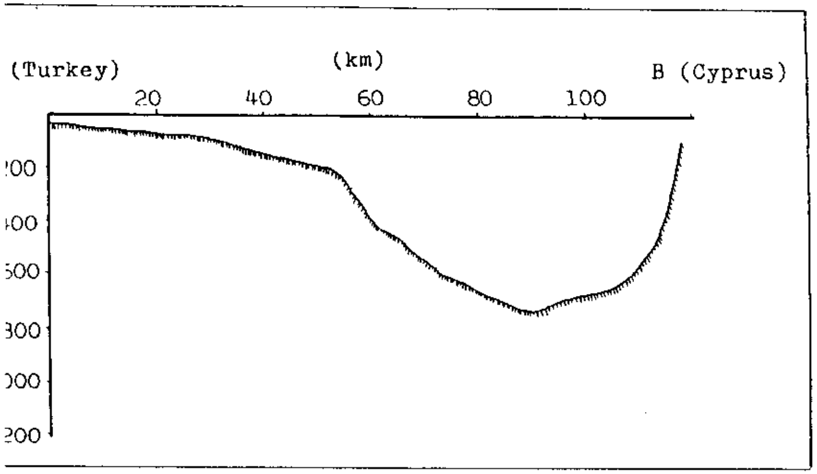

(e)

gure 4.2 Continued

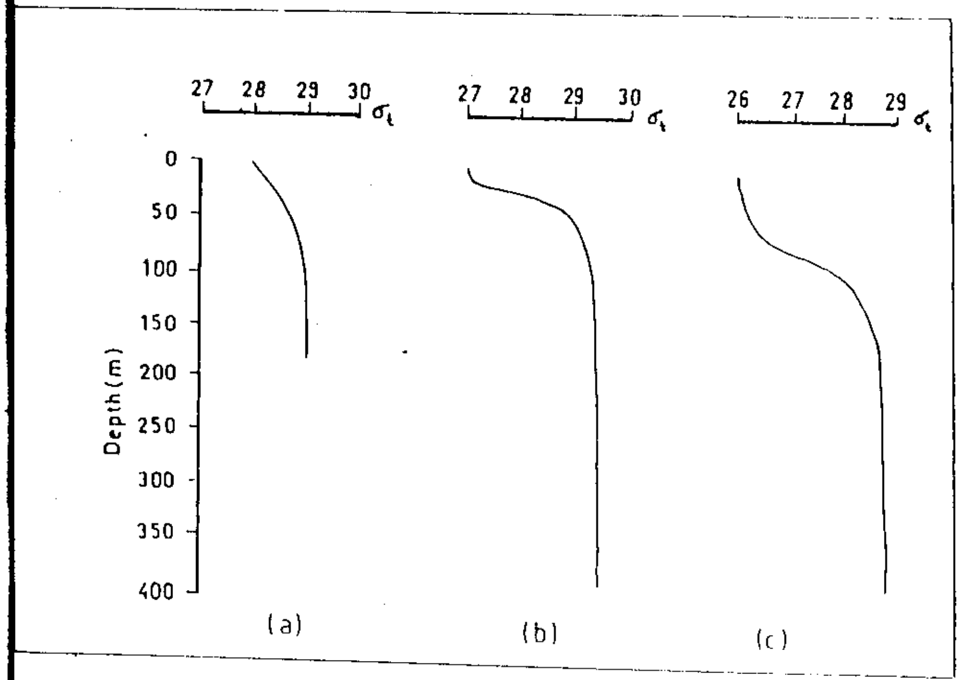

Figure 4.3 Sigma-t profiles taken in

(a) April 1983, from STA 52

(b) June 1983, from STA B26

(c) September 1983, from STA A35

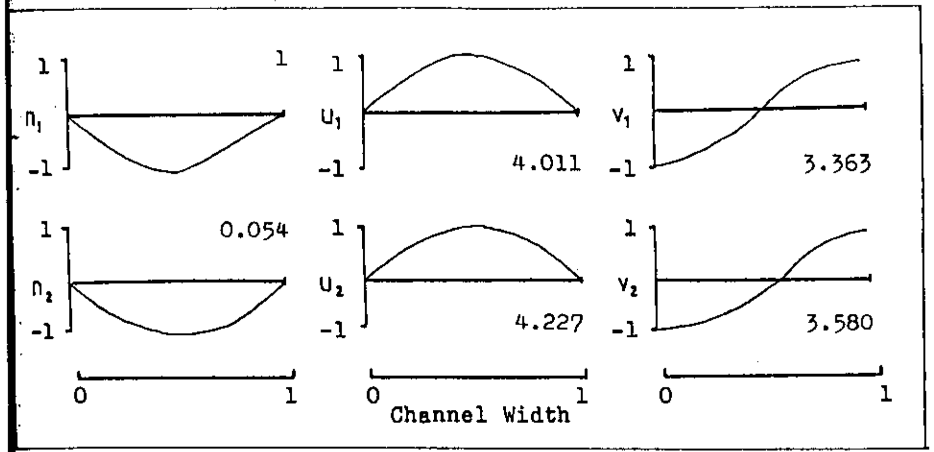

(a)

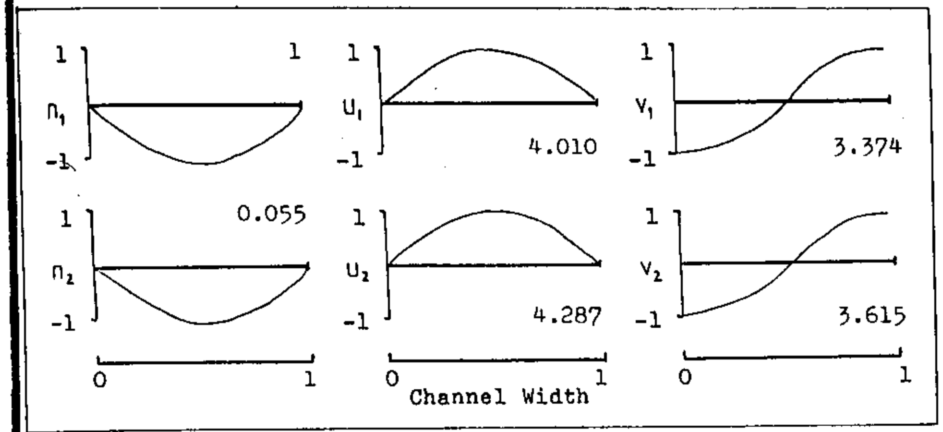

(b)

Figure 4.4 Free surface and interface deformations (η_1, η_2), velocity components for upper (u_1, v_1) and lower (u_2, v_2) layer on an exponential bottom profile, from analytical solution (a), numerical solution (b).

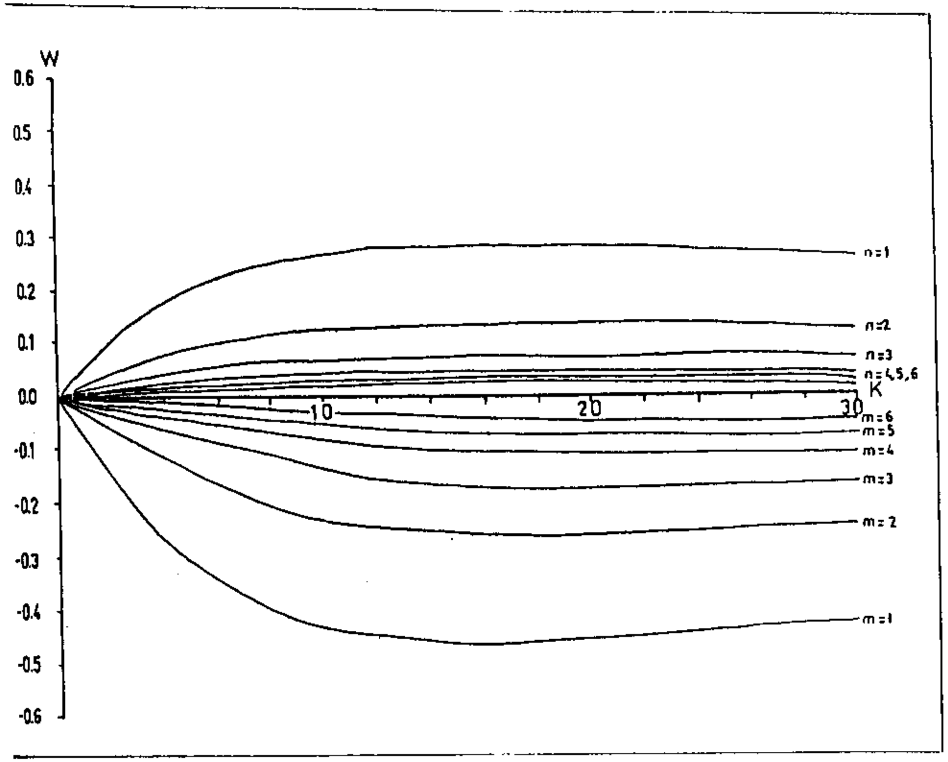

Figure 4.5 Dispersion curves for free modes using one layer model for variable bottom at cross sections A1 (a), A2 (b), A3 (c), A4 (d), A5 (e)

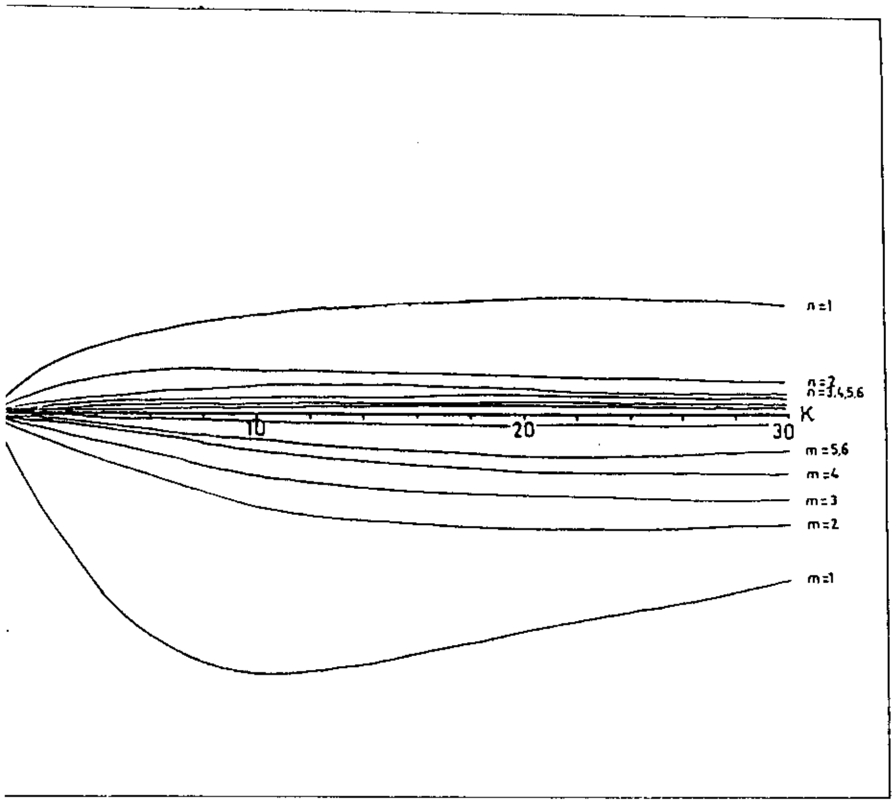

Figure 4.5 Continued (b)

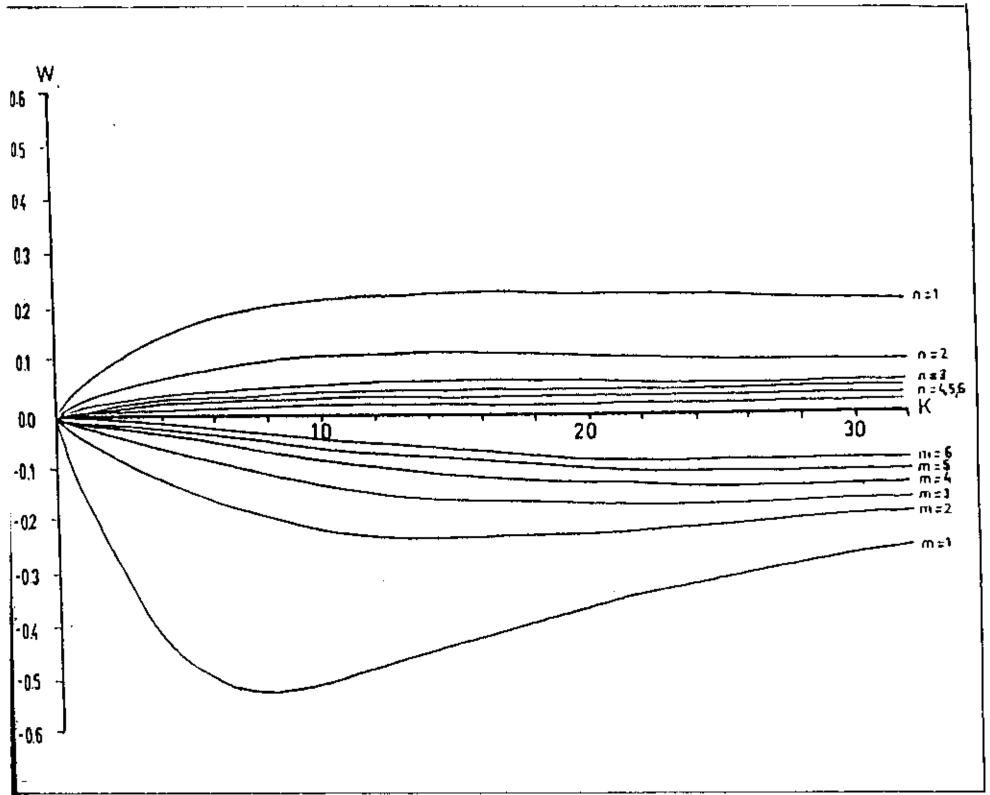

Figure 4.5 Continued (c)

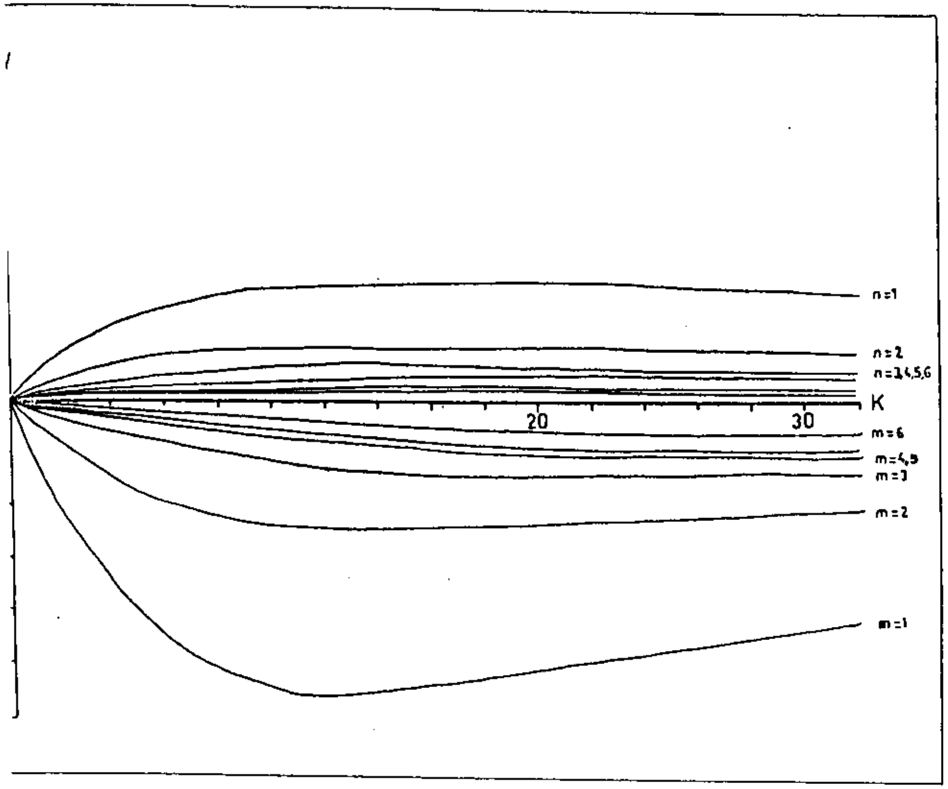

Figure 4.5 Continued (d)

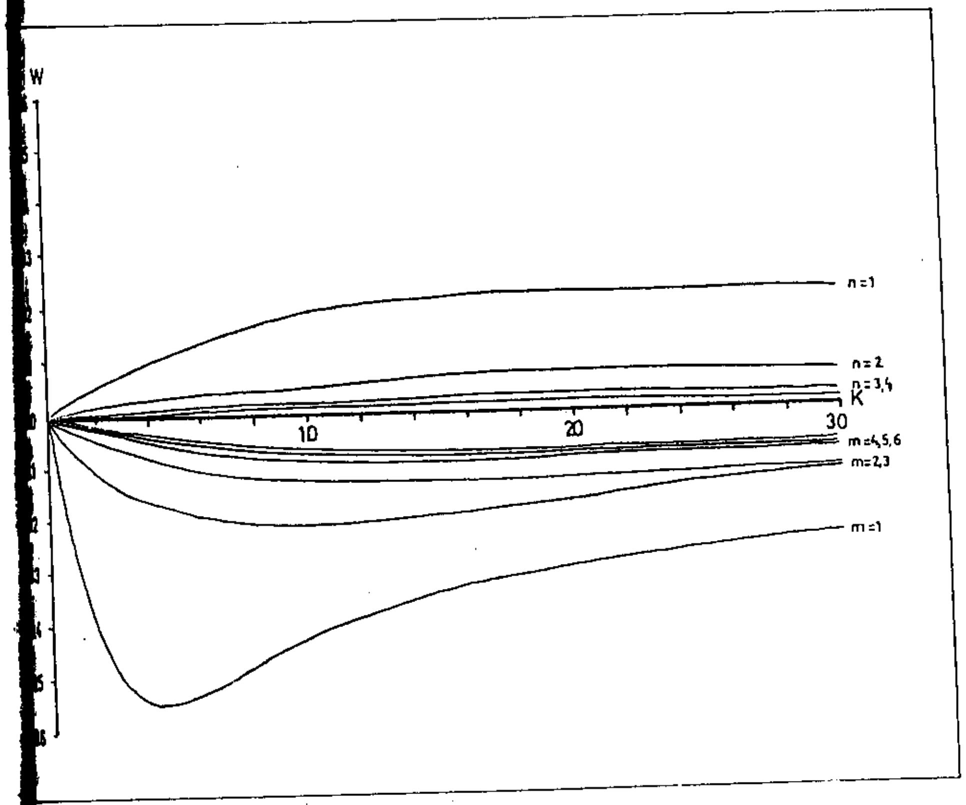

Figure 4.5 Continued (e)

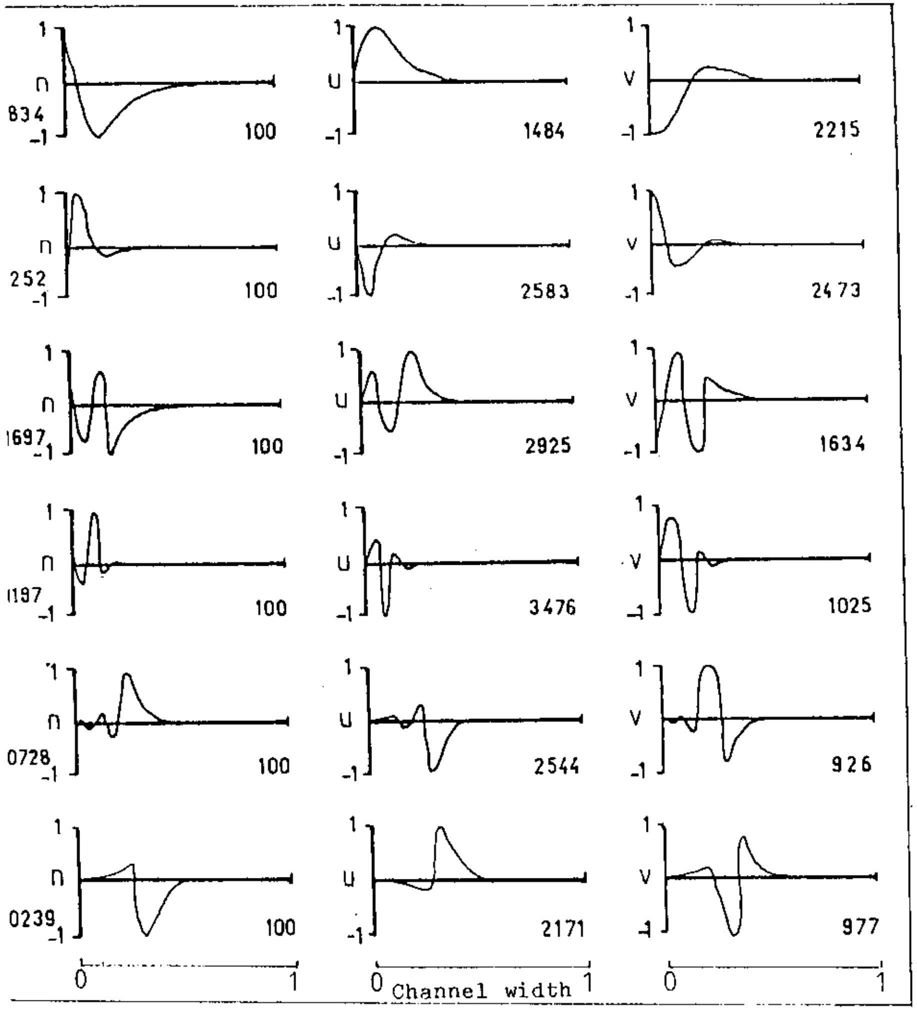

Figure 4.6 Surface deformation (n) and velocity components (u,v) in one layer model.

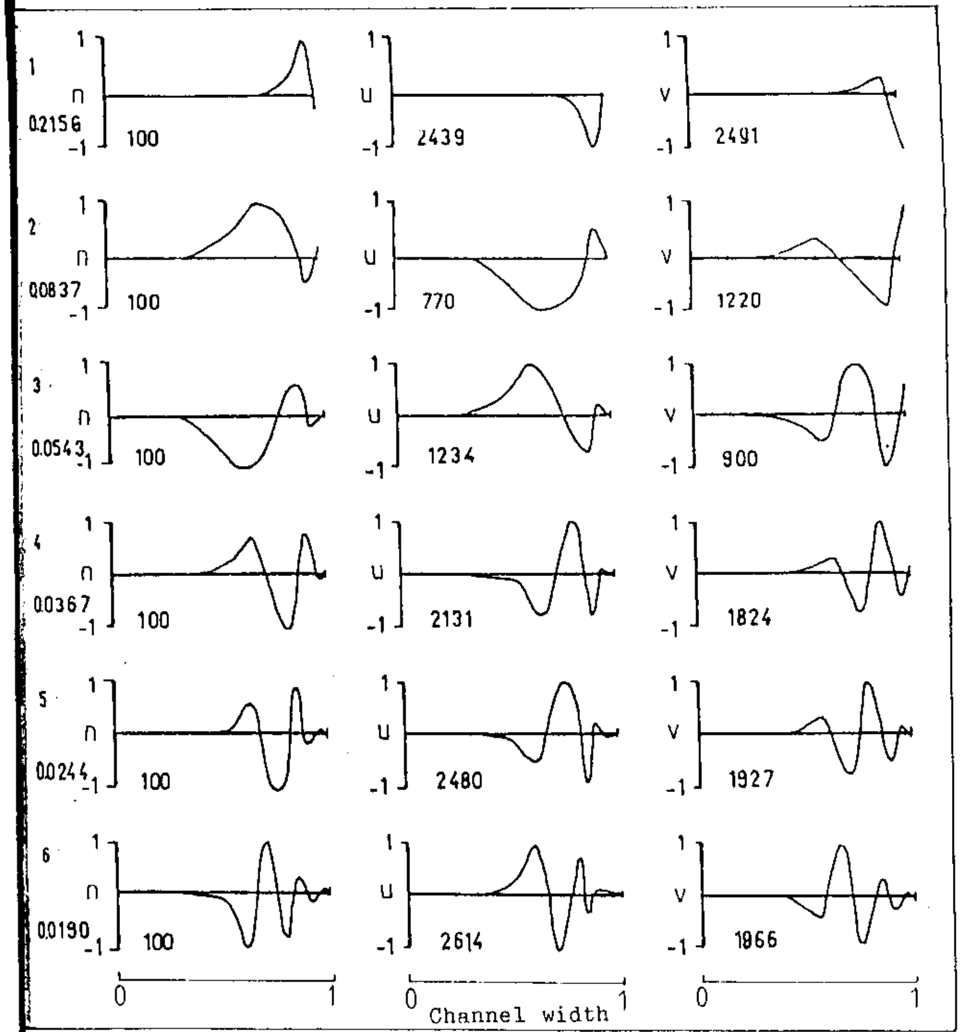

Figure 4.6 Continued

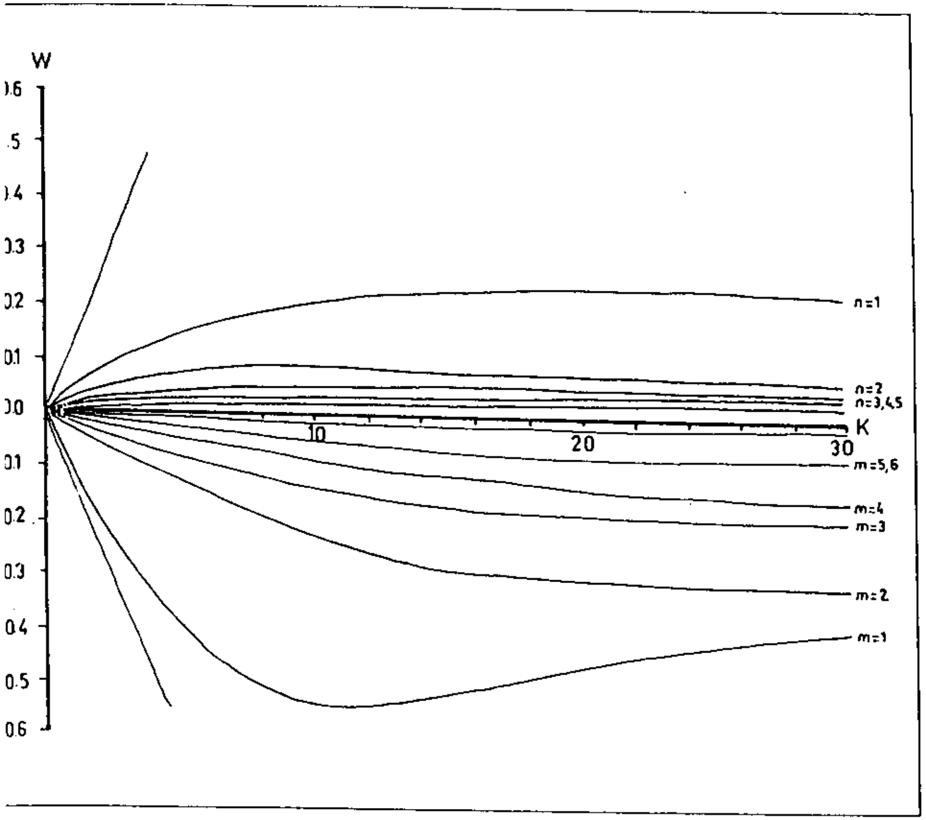

Figure 4.7 Dispersion curves for free modes using two layer model for variable bottom at cross-section A2.

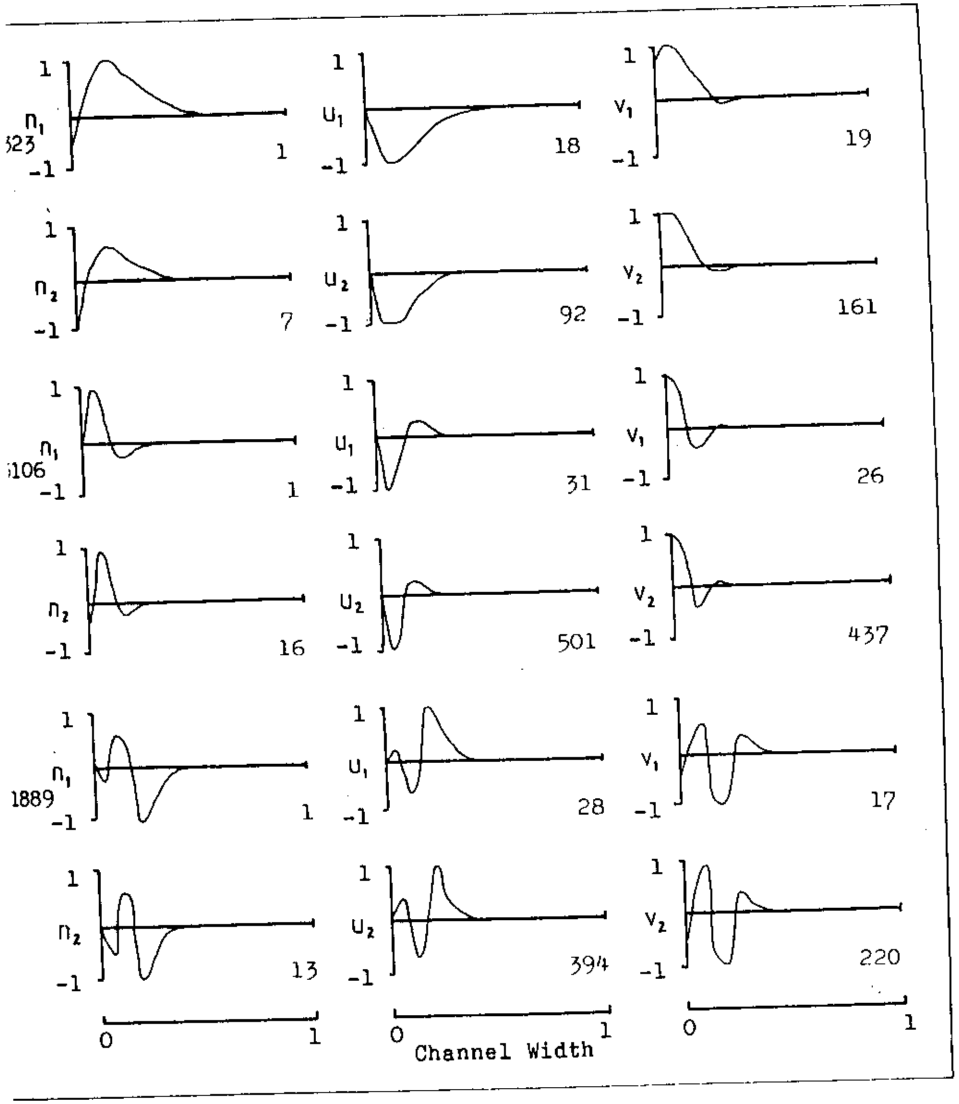

Figure 4.8 Free surface and interface deformations (η_1, η_2), velocity components for upper (u_1, v_1), and lower (u_2, v_2) layers, in two layer model.

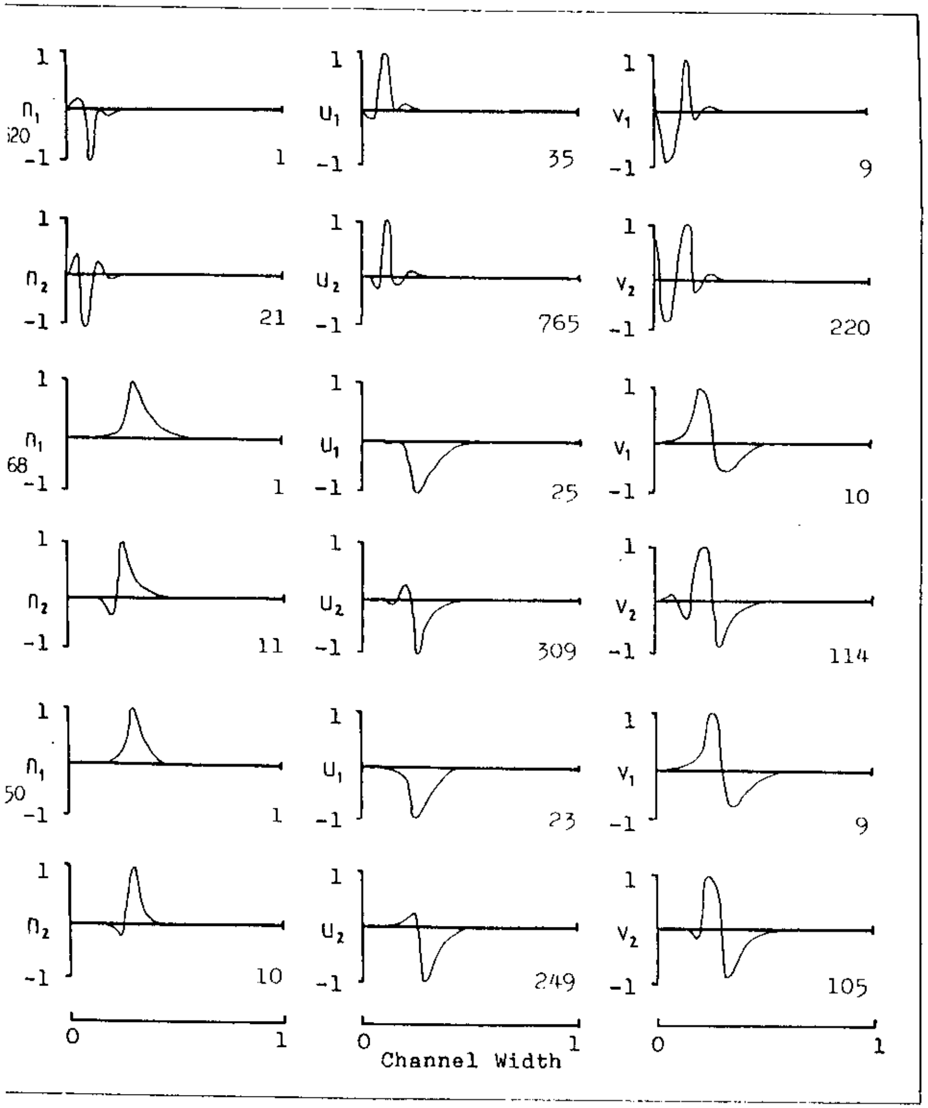

Figure 4.8 Continued

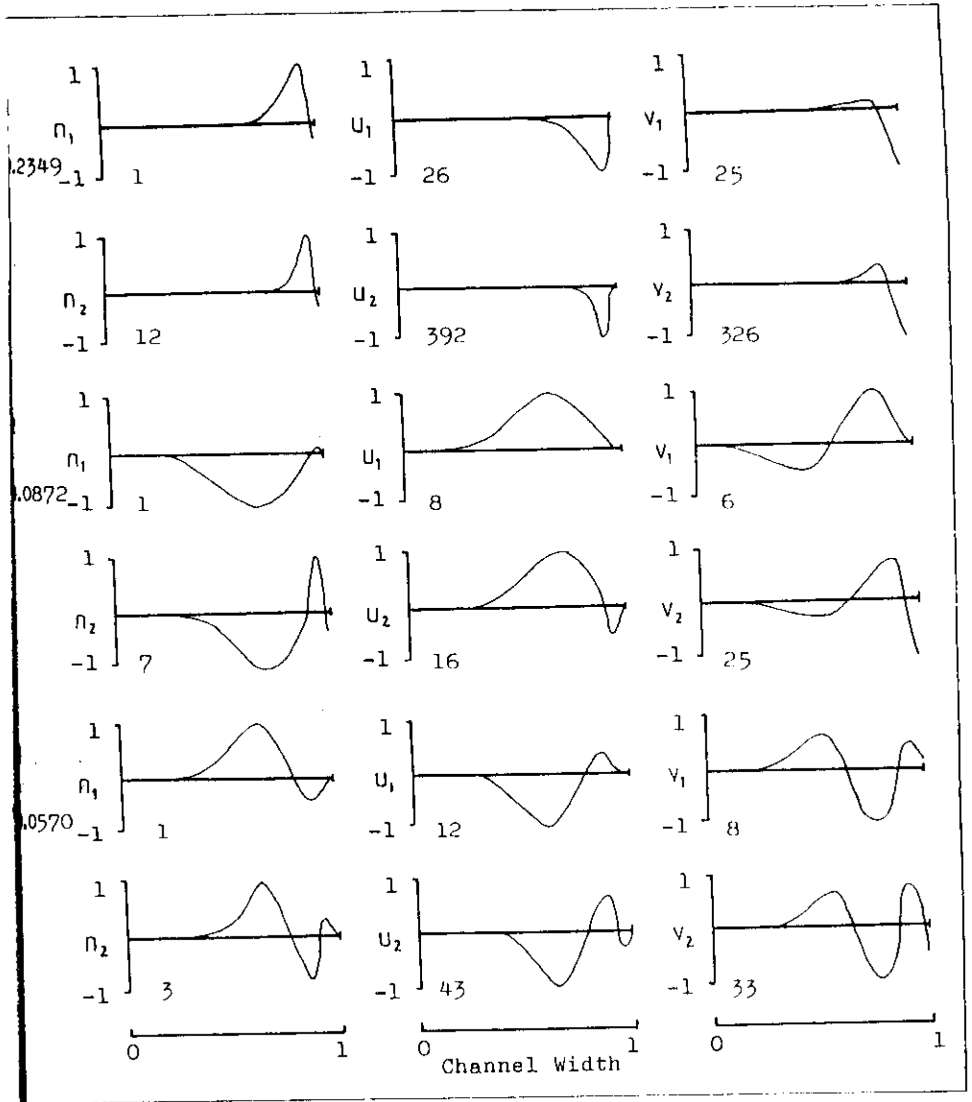

Figure 4.8 Continued

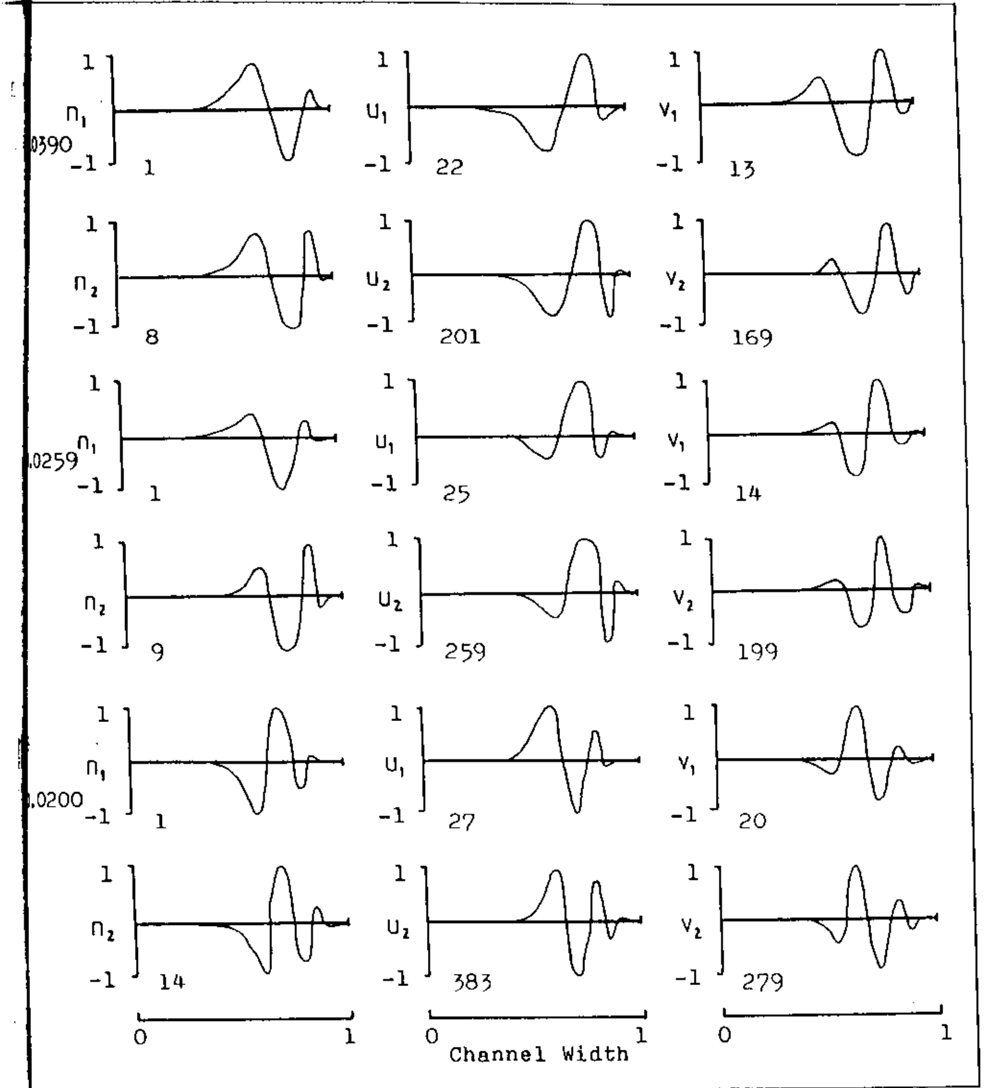

Figure 4.8 Continued

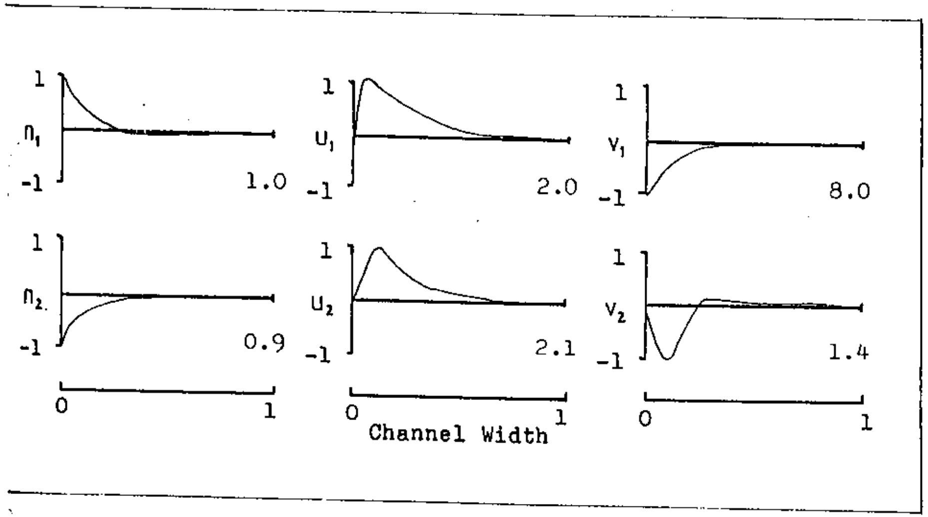

Figure 4.9 Free surface and interface deformations (η_1, η_2) velocity components for upper (u_1, v_1) and lower (u_2, v_2) layer

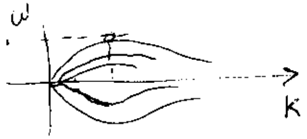

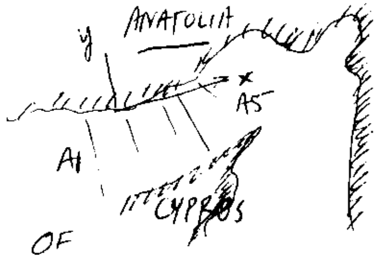

CUTOFF PERIODS OF TOPOGRAPHIC MODES IN THE CILICIAN BASIN

(KIZILKAYA, 1984)

Sections A1-A5

		T (DAYS) 1-LAYER	T (DAYS) 2-LAYER	L (KM) (A2)
C < 0 TURKISH SIDE	1	1.5-1.8	1.1-1.8	48.3
	2	3.3-3.9	2.1-3.2	21.8
	3	4.9-6.3	3.1-4.5	22.5
	4	6.1-8.5	4.7-7.1	16.4
	5	7.4-11.7	5.7-11.1	22.7
	6	8.9-35.6	6.8-34.0	24.2

Section A2

		T (DAYS) 1-LAYER	T (DAYS) 2-LAYER	L (KM)
C > 0 CYPRUS SIDE	1	3.9	3.6	24.7
	2	10.2	9.8	71.7
	3	15.7	14.9	46.3
	4	23.2	21.8	25.3
	5	34.8	32.8	22.0
	6	44.7	42.5	21.0